International Journal of Biological Macromolecules 153 (2020) 608–615

Contents lists available at ScienceDirect

International Journal of Biological Macromolecules

journal homepage: http://www.elsevier.com/locate/ijbiomac

A peroxiredoxin of *Thermus thermophilus* HB27: Biochemical characterization of a new player in the antioxidant defence

Gabriella Fiorentino, Patrizia Contursi, Giovanni Gallo, Simonetta Bartolucci, Danila Limauro *

Dipartimento di Biologia, Università di Napoli Federico II, Complesso universitario di Monte S. Angelo, Via Cinthia, Naples, Italy

ARTICLE INFO

Article history:
Received 3 February 2020
Received in revised form 7 March 2020
Accepted 9 March 2020
Available online 09 March 2020

Keywords:
Peroxiredoxin
Oxidative stress
Thermophiles

ABSTRACT

To fight oxidative damage due to reactive oxygen species (ROS), cells are equipped of different enzymes, among which Peroxiredoxins (Prxs) (EC 1.11.1.15) play a key role. Prxs are thiol-based enzymes containing one (1-Cys Prx) or two (2-Cys Prx) catalytic cysteine residues. In 2-Cys Prxs the cysteine residues form a disulfide bridge following reduction of peroxide which is in turn reduced by Thioredoxin reductase (Tr) /Thioredoxin (Trx) disulfide reducing system to regenerate the enzyme. In this paper we investigated on Prxs of *Thermus thermophilus* whose genome contains an ORF TT_C0933 encoding a putative Prx, belonging to the subfamily of Bacterioferritin comigratory protein (Bcp): the synthetic gene was produced and expressed in *E. coli* and the recombinant protein, *Tt*Bcp, was biochemically characterized. *Tt*Bcp was active on both organic and inorganic peroxides and showed stability at high temperatures. To get insight into disulfide reducing system involved in the recycling of the enzyme we showed that *Tt*Bcp catalically eliminates hydrogen peroxide using an unusual partner, the Protein Disulfide Oxidoreductase (*Tt*PDO) that could replace regeneration of the enzyme. Altogether these results highlight not only a new anti-oxidative pathway but also a promising molecule for possible future biotechnological applications.

1. Introduction

Reactive Oxygen Species (ROS), which include superoxide radical anion (O_2^-) hydrogen peroxide (H_2O_2), hydroxyl radical (HO•), are generated in all aerobic organisms from partial reduction of oxygen. ROS are potent oxidants that damage the main biological macromolecules as proteins, DNA, membrane lipids and can be generated both exogenously (i.e. pollution, UV radiation) and endogenously by the normal oxygen respiration and metabolism (i.e. transport electron chain) [1]. To scavenge ROS every organism has developed efficient antioxidant enzymes involving superoxide dismutase (SOD) that convert O_2^- in H_2O_2 and an array of enzymes that reduce H_2O_2, such as, Peroxiredoxins (Prxs), Glutathione peroxidase and catalase. Prxs (EC 1.11.1.15) are thiol-based enzymes, known to scavenge not only H_2O_2, but also organic peroxides and peroxynitrite [2,3]. In eukaryotes Prxs can also have additional roles because they can be involved in multiple cellular processes like H_2O_2 mediated cellular signalling, protein quality control and associated with cancer, aging, inflammation, neurodegenerative and vascular diseases [4,5]. Generally, the more complex functional role of eukaryotic Prxs compared to prokaryotic ones is ascribed to their higher sensitivity to hyperoxidation due to the presence of conserved Gly-Gly-Leu-Gly (GGLG) and of Tyr-Phe (YF) motives [6,7].

Prx proteins are structurally characterized by a Thioredoxin (Trx) fold [8] in which one or two highly reactive and conserved Cys residues are involved in the reduction of peroxides.

Based on these residues, Prxs are classified in three categories: 1-Cys Prx, atypical 2-Cys Prx, typical 2-Cys Prx. All 2-Cys Prxs contain two conserved residues of cysteine: peroxidatic cysteine (C_P) and the resolving cysteine (C_R) both essential in the catalysis. As reported in Soito et al. [9] Prxs are divided in six subfamilies: Alkyl hydroperoxide reductase C (AhpC)/Prx1, Prx6, Bacterioferritin comigratory protein (Bcp)/PrxQ, Thiol peroxidase (Tpx), Prx5 and Alkyl hydroperoxide reductase E (AhpE). Bcp/PrxQ, generally share a monomeric organization [10] with C_P and C_R located at the N-terminus four residues away from each other. The thiol group of C_P, following the reaction with peroxides, is converted in sulfenic acid (C_PSOH) and establishes an intramolecular disulfide bond with C_R. The regeneration of Prxs is generally resolved by disulfide reductase system that carries electrons from NADPH through Thioredoxin reductase (Tr)/Trx to recycle the active form of the enzyme [11,12].

In the hyperthermophilic archeon *Saccharolobus solfataricus*, it has been shown that a glutaredoxin-like protein, named Protein Disulfide Oxidoreductase (PDO) [13,14], can replace Trx in the redox pair with *Ss*Tr to reduce Prx (Bcp1, Bcp3, Bcp4) [15,16]. It was also suggested that PDOs could play a more complex role contributing to the oxidative folding of thermophilic proteins which are rich in disulfide bonds [17–20] as showed for PDOs of *Pyrococcus furiosus*, *P. horikoshii*,

* Corresponding author.
E-mail address: limauro@unina.it (D. Limauro).

https://doi.org/10.1016/j.ijbiomac.2020.03.052
0141-8130/

Aeropyrum pernix [21–23] and *Aquifex aeolicus* [24]. Recently, a PDO of hyperthermophilic archaeon *Thermococcus onnurineus* NA1 has been characterized and shown to be involved in the transfer of electrons to the terminal acceptor dimethylsulphoxide (DMSO) by reduction of cystine to cysteine [25].

In *T. thermophilus* a monomeric PDO (*Tt*PDO) homologous to *Ss*PDO was characterized; it can be reduced by *Ss*Tr with a good affinity (K_m 34,72 μM) suggesting that a new redox pair exists also in thermophilic bacterium [17].

The aim of this work is to provide more information on the antioxidant system of the thermophilic bacterium *T. thermophilus* HB27, currently not fully clarified [26–29], through the biochemical characterization of the Bcp coded by TT_C0933 [30].

2. Materials and methods

2.1. Bioinformatic analysis

Computation of the theoretical isoelectric point (pI) and molecular weight (Mw) was carried out at website http://www.expasy.org/. Sequence search and homology was carried out using Blasts search tool at NCBI website http://www.ncbi.nlm.nih.gov. Protein Homology/analogY Recognition Engine 2 (Phyre2) (www.sbg.bio.ic.ac.uk/phyre2/) was used to build *Tt*Bcp structural model.

The classification of *Tt*Bcp was carried out using Peroxiredoxin classification index (PREX) database (http://www.csb.wfu.edu/prex). BlastP data base was used to establish % identity between *Tt*Bcp and other homologues (https://blast.ncbi.nlm.nih.gov). Multiple sequence alignment of the amino acids of Prxs was performed using CLUSTAL 2.1.

2.2. Cloning and expression of Ttprx

Based on TT_C0933 DNA sequence, a synthetic gene was commissioned to Eurofins Genomics with the following changes: 1) the codon usage of the gene was optimized for the expression in *Escherichia coli*; 2) *Nde*I and *Hind*III restriction sites were inserted at the 5'end and 3′ ends respectively. The sequence was cloned in the vector pET28b (+) to express a fusion protein with a C-terminal histidine tag. The recombinant vector pET28*Ttbcp* was used to transform *E. coli* strain BL21(DE3) RIL. The transformants were selected on Luria Bertani medium (LB) plates containing ampicillin 50 μg/mL and chloramphenicol 33 μg/mL at 37 °C. A single recombinant clone was inoculated in LB and the culture (1 L) was grown until 0.6 OD at 600 nm before being induced by the addition of 0.5 mM isopropyl-β-D-thiogalactopyranoside (IPTG). The cells were harvested by centrifugation after 16 h incubation at 37 °C; the pellet was suspended in 25 mL of ice-cold 50 mM Tris–HCl pH 7.5 containing a complete EDTA free protease inhibitor cocktail (Roche, IN, USA). After sonication with 10 min pulses at 20 Hz (30 s on and 30 s off), the suspension was clarified by centrifugation at 20000 ×*g* for 1 h at 4 °C.

2.3. Purification of TtBcp

The cytoplasmic extract was subjected to heat treatment at 70 °C for 15 min and then centrifugated at 20000 ×g for 30 min at 4 °C. The supernatant obtained was loaded on the affinity chromatography (HisTrap HP column GE Healthcare, 1 mL), connected to AKTA system, and equilibrated in 50 mM Tris-HCl pH 8.0, 0.5 M NaCl (buffer A). The column was washed with buffer A with 20 mM imidazole, then *Tt*Bcp was eluted with the same buffer A supplemented with 250 mM imidazole [15]. The active fractions were pooled and dialyzed against 20 mM Tris-HCl, pH 8.0. Protein concentration was determined using Bradford assay [31] and protein homogeneity was estimated by SDS-PAGE.

2.4. Size-exclusion chromatography TtBcp

100 μg of purified *Tt*Bcp protein was analyzed by size exclusion chromatography on a Superdex 75 PC (0.3 cm × 3.2 cm) column connected to an AKTA system (GE Healthcare). Proteins were eluted with 50 mMTris-HCl pH 8.0, 0.3 M KCl at a flow rate of 0.04 mL/min. Ovalbumin (43 kDa), RNase A (13.7 kDa) and Aprotinin (6.5 kDa) were used as molecular weight standards (GE Healthcare).

2.5. Circular Dichroism (CD) studies

Far UV CD spectra and thermal denaturation were performed with a J-815 Jasco CD spectropolarimeter, equipped with a Peltier-type temperature control system (model PTC-423S/15). CD measurements were carried out using a quartz cell with a path length of 0.1 cm and 10 μM *Tt*Bcp in 20 mM Na-Phosphate pH 6.8, at different temperatures. Far-UV CD spectra were acquired in 190–250 nm range, with a scan rate continuous, a response of 4 s, 2 nm band width and 0.5 nm data pitch. The signal was averaged over three scans accumulated and corrected by buffer subtraction. CD spectra were analyzed for secondary structure using Dichroweb software (http://dichroweb.cryst.bbk.ac.uk/html/home.shtml) with the Continll program [32].

Thermal stability profile was obtained by recording the CD signal at 222 nm in 30–105 °C temperature range, with a scan rate of 1.0 °C/min.

2.6. Expression, purification and activity assay of TtPDO

*Tt*PDO (locus tag: TTC0486) was expressed in *E. coli* BL21(DE3)RIL/pET-*Ttpdo* and purified as previously reported [17]. *Tt*PDO reductase activity was assayed monitoring the insulin precipitation in presence of 1.2 μM *Tt*PDO [17]. The catalytic reduction of insulin disulfide bonds, due to the insulin chain B precipitation, was followed monitoring the increase in the absorbance at 650 nm, at 30 °C. In detail *Tt*PDO was added in 1 mL reaction mixture containing 100 mM Na-Phosphate pH 7.0, 2 mM EDTA, 1 mg of bovine insulin. A control cuvette contained only the buffer solution and insulin. The reaction started by addition of 1 mM DTT to both cuvettes.

2.7. Expression, purification and activity assay of SsTr

Thioredoxin reductase (locus tag: SSO_RS11745) of *S. solfataricus* (*Ss*Tr) was expressed in *E. coli* BL21(DE3)RIL/pET28TrB3 and purified as reported [14]. The enzymatic activity was determined by 5–5′-dithiobis-(2-nitrobenzoic acid) (DTNB) reduction method [13] where the formation of the product 2-nitro-5-thiobenzoate (TNB) was followed spectrophotometrically by the increase of absorbance at 412 nm. The assay was performed at 60 °C in a reaction mixture containing 0.1 M K-Phosphate buffer pH 7.0, 2 mM EDTA, 0.5 mM DTNB, 0.2 mM NADPH, 0.05 mM FAD, in presence of different concentrations of *Ss*Tr (200–400 nM). To determine the enzymatic activity a molar extinction coefficient of 14,150 M^{-1} cm^{-1} was used.

2.8. Peroxidase activity assays

2.8.1. DTT assay

*Tt*Bcp was tested for its ability to remove peroxides in an in vitro non-enzymatic assay using dithiothreitol (DTT) as reductant to regenerate the reduced enzyme. The mixture containing 50 mM Hepes pH 7.0, 10 mM DTT, *Tt*Bcp 10 μM, was pre incubated for 1 min at 60 °C in a final volume of 0.1 mL. The reaction was carried out at 60 °C for 1 min adding H_2O_2 or tert-butyl hydroperoxide (*t*-BOOH) or cumene hydroperoxide (CHP) at a final concentration of 0.15 mM. The reaction was stopped by adding 0.9 mL of trichloroacetic acid (10%, w/v), as previously described [10]. Peroxidase activity was determined evaluating the amount of remaining peroxide, detected by measurement of the purple-coloured ferrothiocyanate complex at A_{490nm} obtained after

the addition of 0.2 mL of 10 mM $Fe(NH_4)_2(SO_4)_2$ and 0.1 mL of 2.5 M KSCN [10] using relative peroxides as standard. The amount of ferrothiocyanate complex was determined by absorbance at 490 nm. The percentage of peroxides removed was calculated based on the change in A_{490nm} obtained with *Tt*Bcp relative to that obtained without *Tt*Bcp. Experiments were performed in triplicate.

2.8.2. NADPH assay

Peroxidase activity of *Tt*Bcp was also measured indirectly by oxidation of NADPH using a disulfide reductase system constituted by *Ss*Tr/*Tt*PDO [17]. The complete reaction mixture contained 100 mM K-Phosphate pH 7.0, 2 mM EDTA, 0.05 mM FAD, 2 μM *Ss*Tr, 50 μM *Tt*PDO, 0.25 mM NADPH, 5 μM *Tt*Bcp. Different concentrations of H_2O_2 were used (0–1000 μM). After pre-incubation at 60 °C for 5 min, the reaction was started by adding H_2O_2 and the absorbance of NADPH was monitored spectrophotometrically at 340 nm at the same temperature. The activity was determined, after subtracting the reduction rate measured without *Tt*Bcp, using NADPH ε_{340} of 6220 M^{-1} cm^{-1} The data were analyzed by non-linear regression using GraphPad Prism6 program and presented as means of values obtained in triplicate.

2.9. Thermophilicity and thermoresistance

Thermophilicity of *Tt*Bcp was evaluated in the temperature range 40–90 °C by measuring peroxidase activity by the ferrithiocyanate method as previously reported using H_2O_2 as substrate. *Tt*Bcp thermoresistance was estimated by measuring the residual peroxidase after heat treatment at 80 °C, 90 °C, 95 °C for different times by the DTT assay as previously described.

2.10. DNA protection assay

The ability of *Tt*Bcp to protect plasmid DNA against oxidative stress generated by metal ion catalyzed oxidation (MCO) [15] was analyzed as reported below. A reaction mixture of 50 μl included: 50 mM Hepes pH 7.0, 3 μM $FeCl_3$, 10 mM DTT, *Tt*Bcp [2–20 μM]. The reaction was initiated by incubating the mixture for 40 min at 37 °C before adding 2 μg of plasmid pUC18 and incubating for an additional 30 min at the same temperature. The reaction was stopped by adding 3.3 mM EDTA. DNA bands were evaluated on 0.8% (w/v) agarose gel after staining with ethidium bromide 5 μg/mL.

3. Results and discussion

3.1. Bioinformatic analysis

T. thermophilus HB27 genome database [30] contains an open reading frame of 477 nucleotides, (TT_RS04720), encoding a putative Prx (*Tt*Bcp) of 158 amino acids (ID: WP_011173357.1) with a theoretical pI/Mw: 6.84/17537.06.

CLUSTAL 2.1 multiple sequence alignment highlighted conservation of two cysteine residues at position 46 and 51 in the highly conserved region at the N-terminal of *Tt*Bcp, suggesting that it is a 2-Cys Prx which could adopt a reaction mechanism characteristic of Prxs belonging to PrxQ/Bcp subfamily [9] (Fig. 1). In addition, similarly to Bcp1 of *S. solfataricus* (46%identity) [16], the residues highly conserved, underlined in Fig. 1, could delimit a cavity in which the presence of Lys41 and Arg121 provide a positively charged environment to the peroxidatic cysteine (C_P 46).

A structural model was carried out using Phyre2 and crystal structure of an alkyl hydroperoxide reductase from *Burkholderia ambifaria* (PDB c5enuB) as template. The model reported in Fig. 2 shows the presence of Trx fold, common to all Prxs, that consists of a four-stranded β-sheet surrounded by three α-helices with additional secondary structure elements [8].

BlastP analysis showed that *Tt*Bcp shares high identity levels with Prxs of other thermophilic microorganisms. *Tt*Bcp has 80% and 51% identity with Prxs of *Marinithermus hydrothermalis* (WP_013703963.1) and *Thermoanaerobacterium thermosaccharolyticum* (WP_015311480.1) respectively. Moreover, comparable % of identity was highlighted among *Tt*Bcp and Prxs from the pathogenic mesophilic bacteria and (*Helicobacter pullorum* 56%, *Corynebacterium bovis* 52%, *Mycobacterium gordonae* 52%) (Fig. 1).

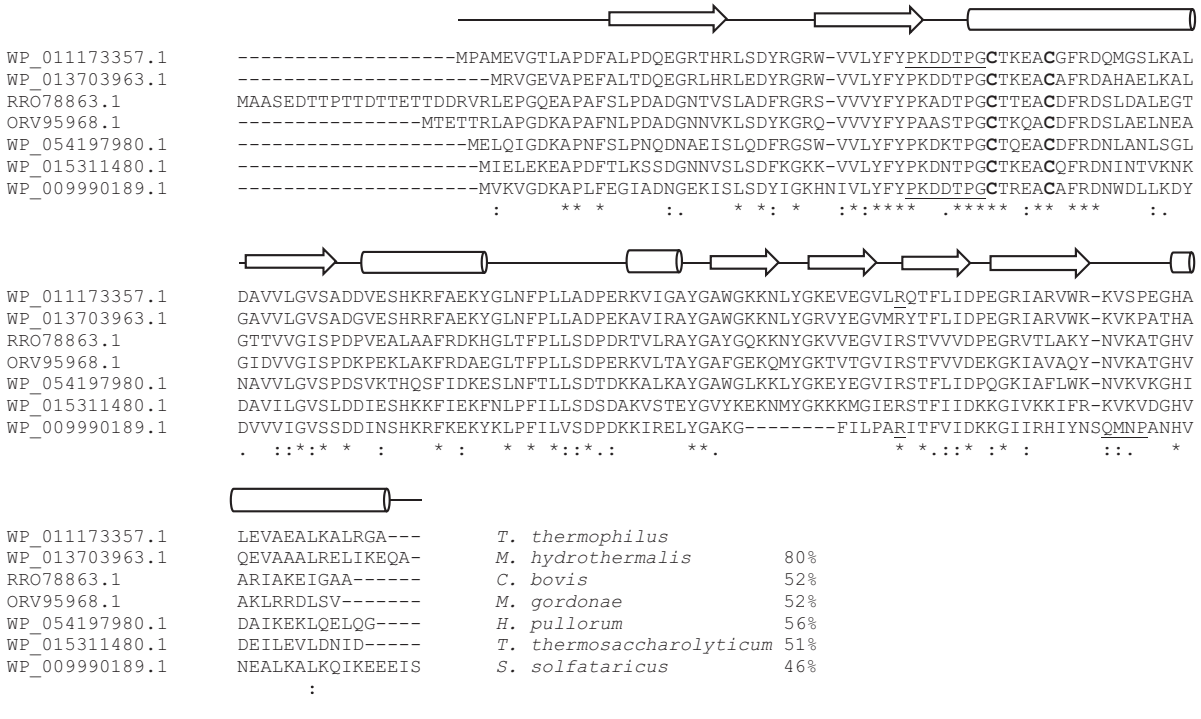

Fig. 1. CLUSTAL 2.1 multiple sequence alignment of *Tt*Bcp with other members belonging to PrxQ/Bcp family. Conserved catalytic Cys residues in positions 46 (peroxidatic cysteine) and 51 (resolving cysteine) are shown in bold. Numbering is referred to *T. thermophilus* sequence; Prx accession numbers are reported on the left, %identity on the right. Above the alignment are indicated secondary sequence elements.

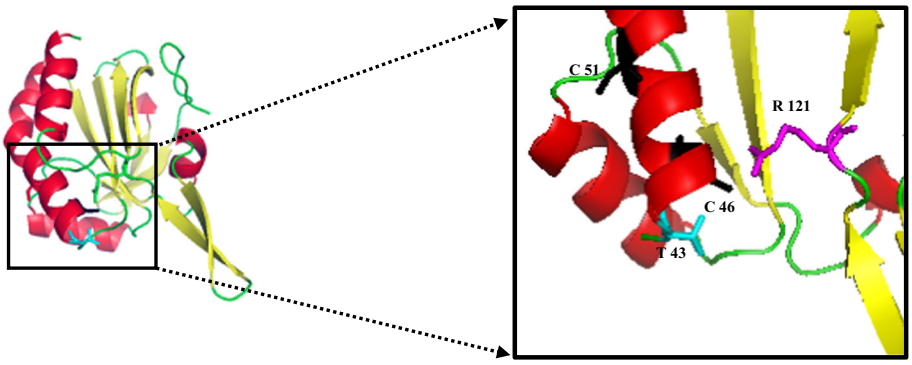

Fig. 2. 3D structure model of *Tt*Bcp. A) The structural model was performed by Phyre2 using as template the crystal structure of an alkyl hydroperoxide reductase from *Burkholderia ambifaria* (PDB n: c5enuB). B) The zoomed picture shows the active site with amino acids involved in the catalysis: T43 (cyano), C46 (black), R121 (magenta), C51 (black).

3.2. Expression, purification and analysis of the quaternary structure of TtBcp

Ttbcp, synthetically produced, was cloned into pET28b vector (pET28*Ttbcp*) and expressed in the *E. coli* BL21(DE3)RILstrain. The protein was purified through a two-step procedure: a thermal precipitation at 70 °C and an IMAC chromatography on His-trap column. The final amount obtained was of 12 mg per liter of bacterial culture. The homogeneity of the purified protein was checked by SDS-PAGE (Fig. 3A). The results showed that the recombinant protein has a MW of approximatively 19,000 Da in agreement with that predicted, considering also the presence of the AAALEHHHHHH sequence fused at C-terminus (19,056,76 Da).

To establish *Tt*Bcp quaternary structure, the protein was analyzed by size exclusion chromatography on a Superdex 75 PC using a calibration curve (insert in Fig. 3B): the molecular mass was estimated to be 15.708 kDa according with a monomeric structure (Fig. 3B) suggesting that the protein belongs to monomeric atypical 2-Cys Prx. This result agrees with most of the characterized enzymes belonging to Bcp/PrxQ subfamily, where the only Bcp with a different structure is the dimeric Bcp4 from *S. solfataricus* [10].

3.3. Circular Dichroism studies

To assess *Tt*Bcp thermal stability, structural studies by CD were performed. Far UV spectra were recorded in the 190–250 nm region at 25 °C, 50 °C and 80 °C to evaluate the influence of the temperature on the secondary structure of the protein. All recorded spectra showed a similar overall shape, suggesting that increased temperature has negligible on the protein secondary structure. The spectra have a maximum at 195 nm and a negative peak at 208 nm (Fig. 4A), revealing the presence of both alfa and beta secondary structure elements. A quantitative estimation of the secondary structure content recorded at 25 °C, was carried out using the DichroWeb software (CDSSTR set 4 program): the α-helix, the β-strand, turns, and unordered structure contents were 13.3%, 34.4%, 21.4%, 30.9%, respectively. Similar values were obtained from the spectra analysis recorded at 50 °C and 80 °C, suggesting that the protein is highly stable.

The thermal stability of the protein was also analyzed measuring the CD signal change at 222 nm in the temperature range between 60 °C and 105 °C. The thermal denaturation, showed in Fig. 4B, was reversible with a Tm of 94 °C, confirming the high thermostability of the protein.

3.4. Functional characterization of TtBcp peroxidase activity

3.4.1. TtBcp peroxidase activity

The peroxidase activity of *TtBcp* towards various substrates was examined by comparing the reduction of three different peroxides: H_2O_2, *t*-BOOH and CHP. Peroxidase activity was measured using DTT as electron donor for enzyme recycling; the amount of remaining peroxide was detected by measurement of the purple-coloured ferrithiocyanate complex

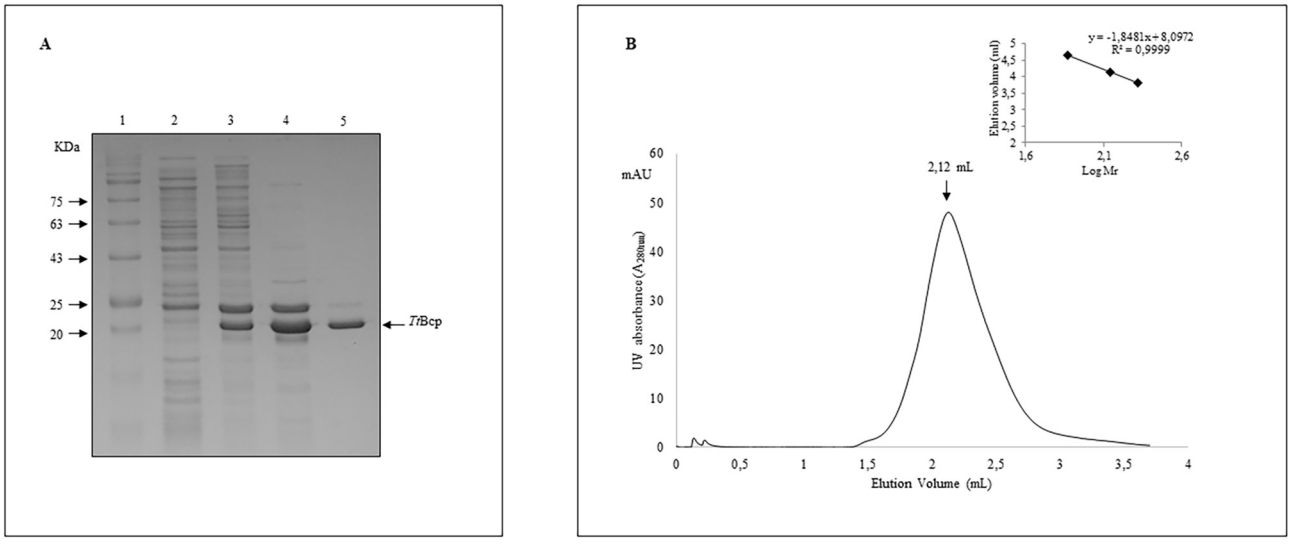

Fig. 3. Purification and analysis of quaternary structure of *Tt*Bcp. A) SDS analysis of *Tt*Bcp purification steps: lane 1) molecular marker; lane 2) cellular extract; lane 3) cellular extract from IPTG - induced cells; lane 4) cellular heat treated extract; lane 5) purified *Tt*Bcp after His-trap chromatography. B) Analysis of *Tt*Bcp by S-75 gel filtration chromatography. Inset (top right): molecular weight standard curve.

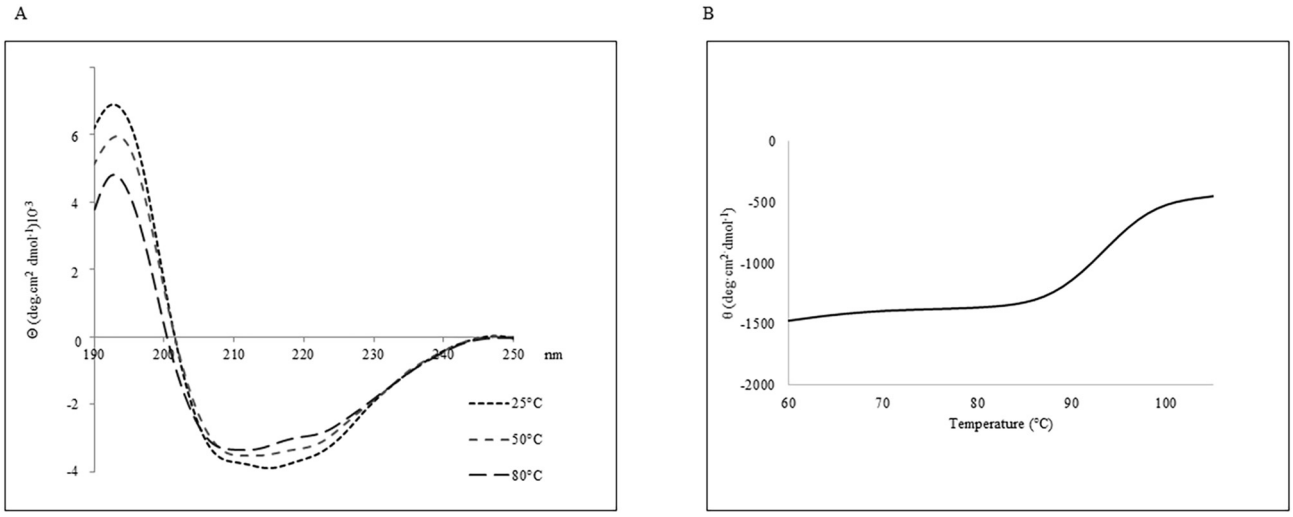

Fig. 4. CD studies of *Tt*Bcp. A) Far-UV CD performed at 25 °C (——), 50 °C (- - - - -) and 80 °C (— — —). The protein concentration to acquire the spectra was 10 mM B) Thermal denaturation curve obtained by recording the changes in molar ellipticity at 222 nm in the temperature range between 60 °C and 105 °C.

at 60 °C, a temperature value at which all the peroxides are still stable. As showed in Fig. 5, *Tt*Bcp was able to reduce all the peroxides tested; the maximum activity was established versus CHP followed by H_2O_2 and *t*-BOOH as for the PrxQ of *Synechocystis* [33] and *C. glutamicum* [34].

3.4.2. TtBcp peroxidase activity using TtPDO as electron donor

To gain insight into the redox system to regenerate *Tt*Bcp in *T. thermophilus*, a thermophilic disulfide reductase hybrid system was used [17]. Heterologous couples for recycling Prxs have already been used for the regeneration of different enzymes: for istance, Tr and Trx of the yeast have been utilized to recycle both Prx2 of mammals [35] and Bcp1 of *S. solfataricus* [36]. Furthermore, the heterologous electron donor pair, *Ss*Tr of *S. solfataricus* and Trx of *E. coli*, has been employed to reduce disulfide bond of the arsenic reductase (ArsC) of *T. thermophilus* [37]. Based on these evidences, the redox pair constituted by *Ss*Tr, that shows a 37% identity with putative *Tt*Tr (WP_011173929) of *T. thermophilus*, and *Tt*PDO [17], was analyzed to regenerate *Tt*Bcp.

*Ss*Tr and *Tt*PDO were purified and their enzymatic activity were measured in independent assays as reported in materials and methods (data not shown); therefore, the peroxidase activity of *Tt*Bcp in the presence of H_2O_2 [0–1000 μM] and NADPH/*Ss*Tr/*Tt*PDO system was measured at 60 °C following the decrease in the absorbance of the NADPH at 340 nm. The determined kinetic parameters suggest that *Tt*PDO is one of the partners involved in the recycling of *Tt*Bcp (Fig. 6). Table 1 reports kinetic parameters determined for *Tt*Bcp in comparison to those of other Bcp/Prx previously measured. The results show a good affinity vs H_2O_2 of *Tt*Bcp with a K_m value comparable to that of *E.coli* Bcp [38] and lower than that PrxQ of *Poplar* [39] and Prx of *C. glutamicum* [34]; in addition *Tt*Bcp has a higher catalytic efficiency the other Prxs. However, it can be hypothized that *Tt*Bcp catalytic efficiency could be even higher using a homologous system and considering that the enzymatic assay was performed under non optimal conditions (redox system and temperature, see below).

These results suggest that *Tt*Bcp could play a key role in the defence against peroxides contributing with other H_2O_2 detoxification enzymes such as Mn catalase of *T. thermophilus* HB8 [26–28,40] to face off oxidative stress.

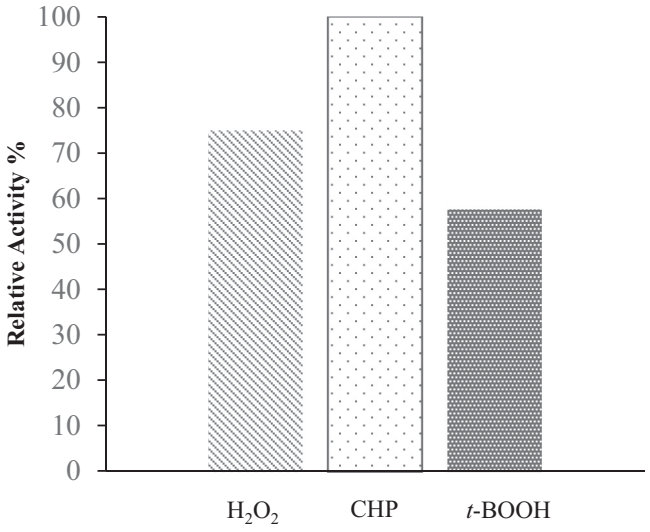

Fig. 5. Substrate specificity of *Tt*Bcp. The peroxidase activity of *Tt*Bcp versus H_2O_2, *t*-BOOH and CHP was measured at 60 °C in presence of DTT by ferrothiocyanate colorimetric assay.

3.5. Effect of temperature on TtBcp peroxidase activity

The effect of temperature on the activity and stability of *Tt*Bcp was determined using DTT assay in presence of H_2O_2 as substrate. The optimum temperature for enzymatic activity resulted to be 80 °C, whereas

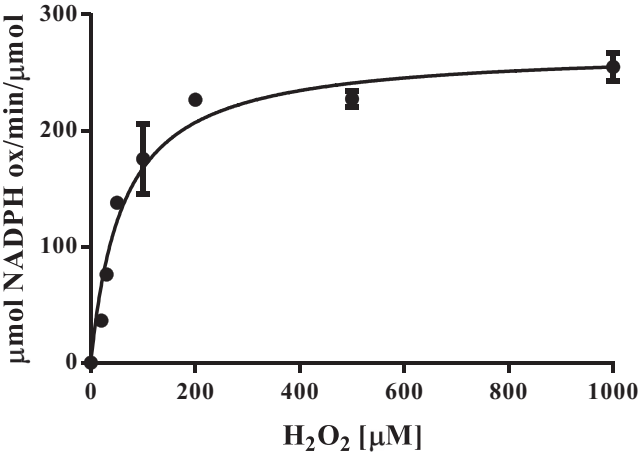

Fig. 6. Michaelis–Menten plot of *Tt*Bcp using H_2O_2 as substrate. The peroxidase was measured using NADPH/*Ss*Tr/*Tt*PDO coupled system, determining the consumption of NADPH via a decrease in absorbance at 340 nm.

Table 1
Kinetics parameters of *Tt*PDO-dependent activity of *Tt*Prx vs H_2O_2 compared to other Prxs belonging PrxQ/Bcp family.

	K_m (μM)	k_{cat} (s^{-1})	k_{cat}/K_m (10^3 M^{-1} s^{-1})	V_{max} (μmol NADPH ox min^{-1} μmol^{-1})
*Tt*Bcp	61.36 ± 8.836	0.91	14.6	270.6
PrxQ *Poplar* [37]	367 ± 37.5	2.93	7.98	176
Bcp *E.coli* [36]	47.8	n.d.	2.45	7.01
Prx *C. glutamicum* [26]	220.9 ± 28.1[a]	2.11 ± 0.07[a]	9.6[a]	n.d.
	333.4 ± 27.6[b]	1.39 ± 0.03[b]	4.2[b]	

Peroxidase assays were performed with NADPH assay as described in Materials and methods.
n.d.: non detected.
[a] Trx1 dependent activity of PrxQ.
[b] Trx2 dependent activity of PrxQ.

at 50 °C and 60 °C the enzymatic activity was ~30% and ~40% of its maximum, respectively (Fig. 7A).

The thermostability of *Tt*Bcp was determined, measuring the residual activity after incubation for different times at 60 °C, 70 °C, 80 °C and 90 °C (Fig. 7B). The results showed that the enzyme retains ~50% of peroxidase activity after 240, 160 or 120 min of incubation at 60 °C, 70 °C, or 80 °C respectively. Finally, the enzyme was completely inactivated after 15 min at 90 °C.

*Tt*Bcp temperature optimum was compared with that of *S. solfataricus* Bcp1, Bcp3, Bcp4 [15] and resulted to be more like that of Bcp1 with which *Tt*Bcp shares the highest sequence identity, but very different from Bcp4 that has higher optimum of temperature (95–100 °C) [10] .This difference in the optimal temperature of *Tt*Bcp was ascribed to the difference in the growth temperatures of two microorganisms that are in the range 50–82 °C [41] and 60–92 °C [42] for *T. thermophilus* and *S. solfataricus* respectively.

3.6. DNA defence of TtBcp from oxidative damage

To evaluate the antioxidant activity of *Tt*Bcp on damaged DNA, pUC18 plasmid DNA was incubated with increasing amount of *Tt*Bcp in the presence of a nicking solution represented by metal-catalyzed oxidation (MCO) system and its mobility analyzed by agarose gel electrophoresis (Fig. 8). The assay was based on the ability to protect plasmids against reduction of O_2 to H_2O_2, catalyzed by Fe^{3+} in the presence of DTT as electron donor. Via the Fenton reaction, the H_2O_2 formed in these conditions was further converted into ·OH, which nicks supercoiled plasmid DNA. As shown in Fig. 8 (lane 1) in the absence of *Tt*Bcp plasmid DNA was converted in nicked form by oxidative damage generated by MCO system, otherwise *Tt*Bcp (lane 3–5) preserved the supercoiled DNA plasmid in a concentration dependent manner. However, as shown in Fig. 8, the supercoiled DNA plasmid is not completely protected, this is probably due to the temperature of the assay (37 °C) that is far from optimal temperature of the enzyme. Nevertheless, these results highlight the role of *Tt*Bcp in DNA protection as also showed for different Prxs-Q and Bcps characterized in various microorganisms [15,42,43].

4. Conclusions

Prxs are enzymes of great relevance for their various functions and properties. From an evolutionary point of view Prxs have been found from the archaea to man; they belong to the Trx subfamily [8] that is characterized by the Trx fold, a scaffold which has proven to be a winner during the evolution for the maintenance of cellular redox homeostasis.

In this work we have demonstrated both the peroxidase activity of *Tt*Bcp and its ability to reduce peroxides using a novel redox pair represented by Tr/PDO, highlighting a new possible physiological role of *Tt*PDO in the antioxidant Bcp system of *T. thermophilus* HB27. Until now, this reductase disulfide system was described only in the archaeon *S. solfataricus*. PDOs are present exclusively in thermophilic microorganisms [21–24] and are characterized by two Trx folds with reductase, oxidase and isomerase activities.

Prxs are very attractive for possible biotechnological application, recently Bcp1 from *S. solfataricus*, particularly thermostable and resistant to extremes pH has been linked on probiotic spores of *Bacillus megaterium* and it has been shown that it maintains its antioxidant activity [44]; it is therefore conceivable that they can be used in drug

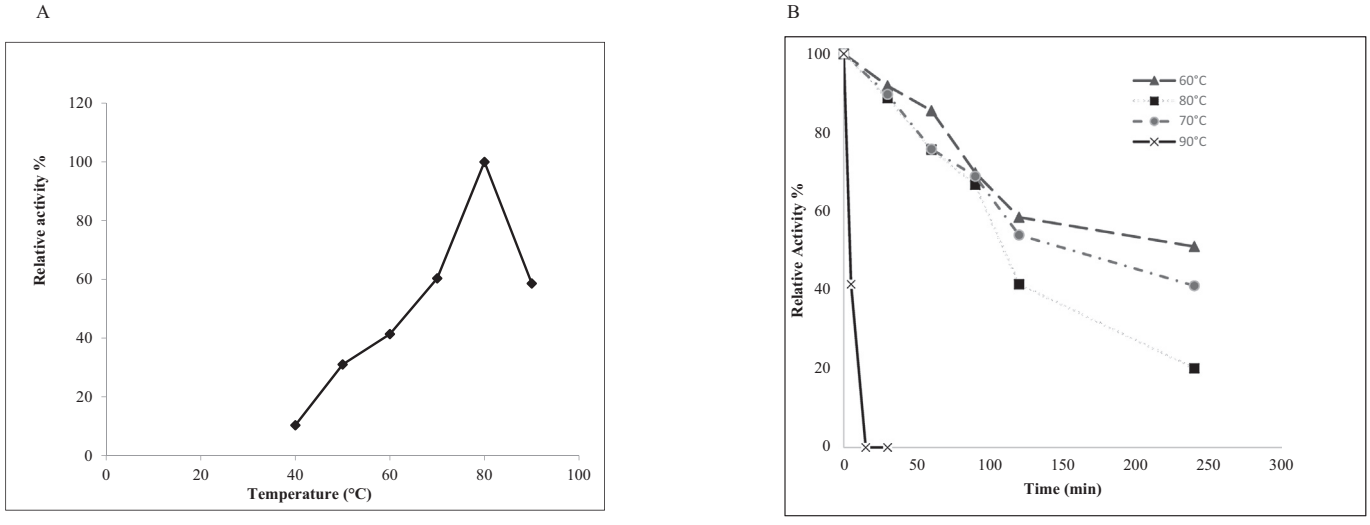

Fig. 7. Effect of temperature on *Tt*Bcp enzymatic activity. A) Temperature optimum was determined in the temperature range 40–90 °C. B) Thermostability was determined as residual activity (%) at 60 °C, 70 °C, 80 °C, 90 °C as function of time. The peroxidase activity versus H_2O_2 was measured by DTT assay.

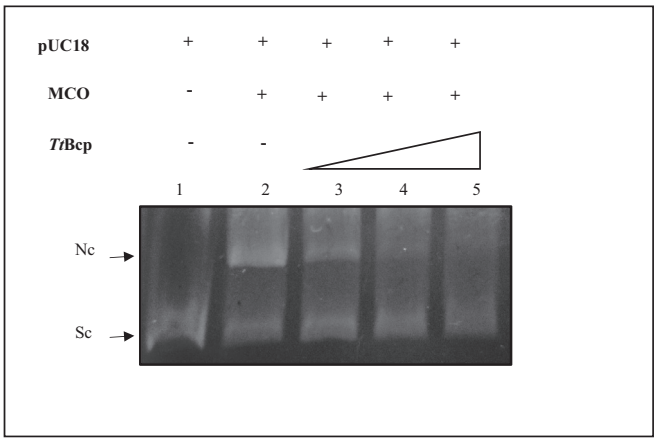

Fig. 8. *Tt*Bcp protection assay of plasmidic DNA in Metal ion Catalyzed Oxidation (MCO) system. Lane 1: plasmid pUC18; lane 2: plasmid pUC18 + MCO system; lane 3: plasmid pUC18 + MCO system + 2 μM *Tt*Bcp; lane 4: plasmid pUC18 + MCO system + 10 μM *Tt*Bcp; lane 5: plasmid pUC18 + MCO system + 20 μM *Tt*Bcp; Sc: Supercoiled form of plasmid, Nc: Nicked form of plasmid.

delivery in pathologies of the inflamed intestine in which ROS are produced. In addition, for thermostable Prxs, such as *Tt*Bcp, it is possible to hypothesize applications in different fields ranging from food to pharmacology to cosmetics.

In conclusion in this work we have not only characterized a new antioxidant enzyme, *Tt*Bcp, involved in the reduction of peroxides but we have identified for the first time in a thermophilic bacterium the peculiar disulfide reductive pathway involving PDO instead of Trx for the regeneration of Bcps.

Funding

This work was supported by Fondo per il Finanziamento delle Attivita' Base di Ricerca (FFABR 2017) Ministero dell'Università e della Ricerca) (MIUR) Italy. Aknowledgements go also to grants from: ERA-NET Cofund MarTERA who funded the project. “FLAshMoB: Functional Amyloid Chimera for Marine Biosensing”; GoodbyWaste: Obtain GOOD products – exploit BY-products – reduce WASTE, MIUR 2017-JTNK78.006, Italy.

Declaration of conflict of interest

The authors declare that there is not conflict of interest.

References

[1] J.A. Imlay, The molecular mechanisms and physiological consequences of oxidative stress: lessons from a model bacterium, Nat. Rev. Microbiol. 11 (2013) 443–454.
[2] L.B. Poole, A. Hall, J.K. Nelson, Overview of Peroxiredoxins in oxidant defense and redox regulation, Curr. Protoc. Toxicol. 7 (Unit 7.9) (2011).
[3] P.A. Karplus, A primer on peroxiredoxin biochemistry, Free Radic. Biol. Med. 80 (2015) 183–190.
[4] M.B. Toledano, B. Huang, Microbial 2-Cys Peroxiredoxins: insights into their complex physiological roles, Mol. Cell 39 (2016) 31–39.
[5] S.G. Rhee, I.S. Kil, Multiple functions and regulation of mammalian peroxiredoxins, Annu. Rev. Biochem. 86 (2017) 749–775.
[6] Y.J. Bang, M.H. Oh, S.H. Choi, Distinct characteristics of two 2-Cys peroxiredoxins of *Vibrio vulnificus* suggesting differential roles in detoxifying oxidative stress, J. Biol. Chem. 287 (2012) 42516–42524.
[7] J.A. Bolduc, K.J. Nelson, A.C. Haynes, J. Lee, J.A. Reisz, A.H. Graff, J.E. Clodfelter, D. Parsonage, L.B. Poole, C.M. Furdui, W.T. Lowther, Novel hyperoxidation resistance motifs in 2-Cys peroxiredoxin, J. Biol. Chem. 293 (2018) 11901–11912.
[8] E. Pedone, D. Limauro, K. D'Ambrosio, G. De Simone, S. Bartolucci, Multiple catalytically active thioredoxin folds: a winning strategy for many functions, Cell. Mol, Life Sci. 67 (2010) 3797–3814.
[9] L. Soito, C. Williamson, S.T. Knutson, J.S. Fetrow, L.B. Poole, K.J. Nelson, PREX: PeroxiRedoxin classification indEX, a database of subfamily assignments across the diverse peroxiredoxin family, Nucleic Acids Res. 39 (2011) D332–D337.
[10] D. Limauro, K. D'Ambrosio, E. Langella, G. De Simone, I. Galdi, C. Pedone, E. Pedone, S. Bartolucci, Exploring the catalytic mechanism of the first dimeric Bcp: functional, structural and docking analyses of Bcp4 from *Sulfolobus solfataricus*, Biochimie 92 (2010) 1435–1444.
[11] J. Lu, A. Holmgren, The thioredoxin antioxidant system, Free Radic. Biol. Med. 66 (2014) 75–87.
[12] A. Holmgren, Thioredoxin, Annu. Rev. Biochem. 54 (1985) 237–271.
[13] E. Pedone, D. Limauro, R. D'Alterio, M. Rossi, S. Bartolucci, Characterization of a multifunctional protein disulfide oxidoreductase from *Sulfolobus solfataricus*, FEBS J. 273 (2006) 5407–5420.
[14] D. Limauro, M. Saviano, I. Galdi, M. Rossi, S. Bartolucci, E. Pedone, *Sulfolobus solfataricus* protein disulphide oxidoreductase: insight into the roles of its redox sites, Protein Eng. Des. Sel. 22 (2009) 19–26.
[15] D. Limauro, E. Pedone, I. Galdi, S. Bartolucci, Peroxiredoxins as cellular guardians in *Sulfolobus solfataricus*: characterization of Bcp1, Bcp3 and Bcp4, FEBS J. 275 (2008) 2067–2077.
[16] K. D'Ambrosio, D. Limauro, E. Pedone, I. Galdi, C. Pedone, S. Bartolucci, G. De Simone, Insights into the catalytic mechanism of the Bcp family: functional and structural analysis of Bcp1 from *Sulfolobus solfataricus*, Proteins 76 (2009) 995–1006.
[17] E. Pedone, G. Fiorentino, L. Pirone, P. Contursi, S. Bartolucci, D. Limauro, Functional and structural characterization of protein disulfide oxidoreductase from *Thermus thermophilus* HB2, Extremophiles 18 (2014) 723–731.
[18] R. Ladenstein, B. Ren, Protein disulfides and protein disulfide oxidoreductases in hyperthermophiles, FEBS J. 273 (2006) 4170–4185.
[19] M. Beeby, B.D. O'Connor, C. Ryttersgaard, D.R. Boutz, L.J. Perry, T.O. Yeates, The genomics of disulfide bonding and protein stabilization in thermophiles, PLoS Biol. 3 (2005), e309.
[20] F. Hatahet, D. Boyd, J. Beckwith, Disulfide bond formation in prokaryotes: history, diversity and design, Biochim. Biophys. Acta 1844 (2014) 1402–1414.
[21] E. Pedone, B. Ren, R. Ladenstein, M. Rossi, S. Bartolucci, Functional properties of the protein disulfide oxidoreductase from the archaeon *Pyrococcus furiosus*: a member of a novel protein family related to protein disulfide-isomerase, Eur. J. Biochem. 271 (2004) 3437–3448.
[22] K. D'Ambrosio, E. Pedone, E. Langella, G. De Simone, M. Rossi, C. Pedone, S. Bartolucci, A novel member of the protein disulfide oxidoreductase family from *Aeropyrum pernix* K1: structure, function and electrostatics, J. Mol. Biol. 362 (2006) 743–752.
[23] B. Ren, G. Tibbelin, D. de Pascale, M. Rossi, S. Bartolucci, R. Ladenstein, A protein disulfide oxidoreductase from the archaeon *Pyrococcus furiosus* contains two thioredoxin fold units, Nat. Struct. Biol. 5 (1998) 602–611.
[24] E. Pedone, K. D'Ambrosio, G. De Simone, M. Rossi, C. Pedone, S. Bartolucci, Insights on a new PDI-like family: structural and functional analysis of a protein disulfide oxidoreductase from the bacterium *Aquifex aeolicus*, J. Mol. Biol. 356 (2006) 155–164.
[25] A.R. Choi, M.S. Kim, S.G. Kang, H.S. Lee, Dimethyl sulfoxide reduction by a hyperhermophilic archaeon *Thermococcus onnurineus* NA1 via a cysteine-cystine redox shuttle, J. Microbiol. 54 (2016) 31–38.
[26] A. Hidalgo, L. Betancor, R. Moreno, O. Zafra, F. Cava, R. Fernández-Lafuente, J.M. Guisán, J. Berenguer, *Thermus thermophilus* as a cell factory for the production of a thermophilic Mn-dependent catalase which fails to be synthesized in an active form in *Escherichia coli*, Appl. Environ. Microbiol. 70 (2004) 3839–3844.
[27] A. Hidalgo, L. Betancor, C. Mateo, F. Lopez-Gallego, R. Moreno, J. Berenguer, J.M. Guisán, R. Fernández-Lafuente, Purification of a catalase from *Thermus thermophilus* via IMAC chromatography: effect of the support, Biotechnol. Prog. 20 (2004) 1578–1582.
[28] R. Moreno, A. Hidalgo, F. Cava, R. Fernández-Lafuente, J.M. Guisán, J. Berenguer, Use of an antisense RNA strategy to investigate the functional significance of Mn-catalase in the extreme thermophile *Thermus thermophilus*, J. Bacteriol. 186 (2004) 7804–7806.
[29] J. Liu, M. Yin, H. Zhu, J. Lu, Z. Cui, Purification and characterization of a hyperthermostable Mn-superoxide dismutase from *Thermus thermophilus* HB27, Extremophiles 15 (2011) 221–226.
[30] A. Henne, H. Brüggemann, C. Raasch, A. Wiezer, T. Hartsch, H. Liesegang, A. Johann, T. Lienard, O. Gohl, R. Martinez-Arias, C. Jacobi, V. Starkuviene, S. Schlenczeck, S. Dencker, R. Huber, H.P. Klenk, W. Kramer, R. Merkl, G. Gottschalk, H.J. Fritz, The genome sequence of the extreme thermophile *Thermus thermophilus*, Nat. Biotechnol. 22 (2004) 547–553.
[31] M. Bradford, A rapid and sensitive method forthe quantification of microgram quantities of protein utilizing the principle of protein-dye binding, Anal. Biochem. 72 (1976) 248–254.
[32] N. Sreerama, R.W. Woody, Estimation of protein secondary structure from circular dichroism spectra: comparison of CONTIN, SELCON, and CDSSTR methods with an expanded reference set, Anal. Biochem. 287 (2000) 252–260.
[33] M.E. Pérez-Pérez, A. Mata-Cabana, A.M. Sánchez-Riego, M. Lindahl, F.J. Florencio, A comprehensive analysis of the peroxiredoxin reduction system in the *Cyanobacterium Synechocystis* sp. strain PCC 6803 reveals that all five peroxiredoxins are thioredoxin dependent, J. Bacteriol. 191 (2009) 7477–7489.
[34] T. Su, M. Si, Y. Zhao, Y. Liu, S. Yao, C. Chen, A thioredoxin-dependent peroxiredoxin Q from *Corynebacterium glutamicum* plays an important role in defense against oxidative stress, PLoS One 13 (2018), e0192674.
[35] J.A. Kim, S. Park, K. Kim, S.G. Rhee, S.W. Kang, Activity assay of mammalian 2-cys peroxiredoxins using yeast thioredoxin reductase system, Anal. Biochem. 338 (2005) 216–223.
[36] C. Sarcinelli, G. Fiorentino, E. Pizzo, S. Bartolucci, D. Limauro, Discovering antioxidant molecules in the Archaea domain: peroxiredoxin Bcp1 from *Sulfolobus solfataricus* protects H9c2 cardiomyoblasts from oxidative stress, Archaea 2016 (2016), 7424870.

[37] I. Del Giudice, D. Limauro, E. Pedone, S. Bartolucci, G. Fiorentino, A novel arsenate reductase from the bacterium Thermus thermophilus HB27: its role in arsenic detoxification, Biochim. Biophys. Acta 1834 (2013) 2071–2079.
[38] W. Jeong, M.K. Cha, I.H. Kim, Thioredoxin-dependent hydroperoxide peroxidase activity of bacterioferritin comigratory protein (BCP) as a new member of the thiol-specific antioxidant protein (TSA)/Alkyl hydroperoxide peroxidase C (AhpC) family, J. Biol. Chem. 275 (2000) 2924–2930.
[39] N. Rouhier, E. Gelhaye, J.M. Gualberto, M.N. Jordy, E. De Fay, M. Hirasawa, S. Duplessis, S.D. Lemaire, P. Frey, F. Martin, W. Manieri, D.B. Knaff, J.P. Jacquot, Poplar peroxiredoxin Q. A thioredoxin-linked chloroplast antioxidant functional in pathogen defense, Plant Physiol. 134 (2004) 1027–1038.
[40] N. Ohtani, M. Tomita, M. Itaya, An extreme thermophile, *Thermus thermophilus*, is a polyploid bacterium, J. Bacteriol. 192 (2010) 5499–5505.
[41] M. Zaparty, D. Esser, S. Gertig, P. Haferkamp, T. Kouril, A. Manica, T.K. Pham, J. Reimann, K. Schreiber, P. Sierocinski, D. Teichmann, M. van Wolferen, M. von Jan, P. Wieloch, S.V. Albers, A.J. Driessen, H.P. Klenk, C. Schleper, D. Schomburg, J. van der Oost, P.C. Wright, B. Siebers, "Hot standards" for the thermoacidophilic archaeon *Sulfolobus solfataricus*, Extremophiles 14 (2010) 119–4226.
[42] S. Lee, J.M. Chung, H.J. Yun, J. Won, H.S. Jung, New insight into multifunctional role of peroxiredoxin family protein: determination of DNA protection properties of bacterioferritin comigratory protein under hyperthermal and oxidative stresses, Biochem. Biophys. Res. Commun. 469 (2016) 1028–1033.
[43] A. Singh, N. Kumar, P.P.S. Tomar, S. Bhose, D.K. Ghosh, P. Roy, A.K. Sharma, Characterization of a bacterioferritin comigratory protein family 1-Cys peroxiredoxin from *Candidatus Liberibacter asiaticus*, Protoplasma 254 (2017) 1675–1691.
[44] M. Lanzilli, G. Donadio, F.A. Fusco, C. Sarcinelli, D. Limauro, E. Ricca, R. Isticato, Display of the peroxiredoxin Bcp1 of *Sulfolobus solfataricus* on probiotic spores of *Bacillus megaterium*, New Biotechnol. 46 (2018) 38–44.